Reproductive Sciences (2020) 27:1411–1422
https://doi.org/10.1007/s43032-019-00108-2

ORIGINAL ARTICLE

# Diagnosing Deep Endometriosis Using Transvaginal Elastosonography

Ding Ding[1] · Yishan Chen[1] · Xishi Liu[1,2] · Zongqin Jiang[3] · Xianjun Cai[3] · Sun-Wei Guo[1,2]

Received: 12 June 2019 / Accepted: 28 August 2019 / Published online: 24 April 2020


## Abstract

Transvaginal ultrasound (TVUS) and MRI are currently two mainstream imaging techniques used to diagnose deep endometriosis (DE) with comparable accuracy, but there is still ample room for improvement. As endometriotic lesions progress to fibrosis concomitant with the increase in tissue stiffness, transvaginal elastosonography (TVESG) is well-suited for diagnosing DE. To test the hypothesis that lesional stiffness as measured by TVESG correlates with the extent of lesional fibrosis, the markers of progression, hormonal receptor expression, and vascularity, we recruited 30 patients suspected to have DE who went through pelvic examination, TVUS and/or MRI, and TVESG and were ultimately diagnosed by histology. Their lesional tissue samples were subjected to immunohistochemistry analysis of markers for epithelial-mesenchymal transition (EMT), fibroblast-to-myofibroblast transdifferentiation (FMT), estrogen and progesterone receptors (ERβ and PR), microvessel density (MVD), and vascularity, as well as quantification of lesional fibrosis. We found that pelvic examination, TVUS, and MRI detected 83.3%, 66.7%, and 83.3% of all DE cases, respectively, while TVESG detected them all. The lesions missed by pelvic exam, TVUS and MRI were significantly smaller than those detected but nonetheless had higher lesional stiffness. Lesional stiffness correlated closely and positively with the extent of lesional fibrosis, negatively with the markers of EMT, MVD, vascularity, and PR expression, but positively with the marker for FMT and ERβ. Thus, through the additional use of information on differential stiffness between DE lesions and their surrounding tissues, TVESG improves diagnostic accuracy, provides a ballpark estimate on the developmental stage of the lesions, and may help clinicians choose the best treatment modality.

**Keywords** Deep endometriosis · Fibrosis · Progesterone receptor · Stiffness · Transvaginal ultrasonography · Transvaginal elastosonography · Vascularity

## Introduction

Deep endometriosis (DE) is one of three major subtypes of endometriosis [1]. Although the prevalence of DE is much lower than that of ovarian endometriomas (OE) [2, 3], most women with DE have severe pain [3]. As such, DE is recognized as the most severe clinical form of endometriosis with challenging clinical management [4].

Currently, transvaginal ultrasound (TVUS) and magnetic resonance imaging (MRI) are two mainstream imaging modalities used to diagnose DE [5, 6]. The imaging techniques can map the locations of DE lesions and help triage patients before surgery. Due to its lower cost than MRI, its ubiquity and the ease of use, TVUS is now the first-line imaging technique in the workup for women with pelvic pain and suspected endometriosis [6, 7], with comparable diagnostic accuracy as that of MRI [8–14]. However, there is still ample room for improvement [6, 15].

Ding Ding and Yishan Chen contributed equally to this work.

**Electronic supplementary material** The online version of this article (https://doi.org/10.1007/s43032-019-00108-2) contains supplementary material, which is available to authorized users.

✉ Xishi Liu
lxsdoc@hotmail.com

Sun-Wei Guo
hoxa10@outlook.com

[1] Shanghai OB/GYN Hospital, Fudan University, Shanghai 200090, China

[2] Shanghai Key Laboratory of Female Reproductive Endocrine-Related Diseases, Fudan University, Shanghai, China

[3] Department of Obstetrics and Gynecology, The 7th Hospital, Ningbo, Zhejiang 315202, China

DE lesions are fundamentally wounds undergoing repeated tissue injury and repair (ReTIAR), progressing to fibrosis through epithelial-mesenchymal transition (EMT), fibroblast-to-myofibroblast transdifferentiation (FMT), and smooth muscle metaplasia (SMM) [16–21]. These new findings explain quite nicely the increased nerve fiber density [22, 23] and fibromuscular content [24, 25] in DE lesions. As in adenomyotic lesions, the extent of fibrosis in DE lesions should correlate with lesional stiffness, which contains information inherently embedded within the lesions, revealing just how advanced the lesion is. Unfortunately, neither conventional TVUS nor MRI can evaluate this quantity.

Yet lesional stiffness can be measured by elastography, which is a recently emerged new imaging technology that generates images of tissue stiffness, mainly by ultrasound (elastosonography or ESG). MRI-based elastography also is on the horizon and will be available in the future. Similar to the ancient technique of palpation, ESG can measure the stiffness of the tissues of interest with better spatial localization information [26]. Currently, there are roughly two different types of ESG: strain imaging and shear-wave imaging [26]. Both types require mechanical excitation, akin to palpation. Strain ESG measures the tissue deformation or displacement generated by applying pressure (as an excitation) with a probe, while shear-wave ESG records the propagation of shear-waves after excitation [27, 28]. In many commercial ESGs, the tissue stiffness is displayed in false-color image, often side by side with the B-mode image, which greatly facilitates the interpretation of imaging results.

In fact, ESG has been proven invaluable to access the extent of fibrosis in liver and to diagnose tumors of the breast and other organs [28, 29]. ESG also has been used in diagnosing endometriosis, including DE [30–35]. While all these studies demonstrated the potentials of ESG in diagnosing DE, very little is known as whether the lesional stiffness has anything to do with the lesional histology.

We have recently used TVESG to diagnose adenomyosis and found it to be superior to conventional TVUS [36]. More remarkably, we found that lesional stiffness correlates positively with uterine size and the extent of fibrosis but negatively with E-cadherin and progesterone receptor (PR) expression levels in lesions [36]. Since adenomyotic lesions are also wounds undergoing ReTIAR [37, 38] just like endometriotic lesions [39], we hypothesized that DE lesions can also be diagnosed with TVESG with more accuracy. In addition, given the relationship between the extent of lesional fibrosis and hormonal receptor expression levels, the thoroughness of EMT, FMT, and the vascularity [40], we hypothesized that the lesional stiffness as measured by TVESG also should correlate with these parameters. This study was undertaken to test these hypotheses.

## Materials and Methods

### Patients and Specimen

Thirty premenopausal patients who visited Shanghai Obstetrics & Gynecology Hospital from March to September, 2018, and were ultimately diagnosed and histologically confirmed with DE were recruited. All of them underwent DE lesion excision surgery and those who also had OE and/or adenomyosis underwent ovarian cystectomy and/or hysterectomy as well according to patients' wishes and the indications. To rule out the possible effect of hormonal treatment on diagnostic accuracy, we deliberately excluded patients who had taken hormonal treatment prior to the surgery. Therefore, none of the recruited patients received any hormonal treatment 3 months prior to the surgery. This study was approved by the Institutional Ethics Review board of Shanghai Obstetrics & Gynecology Hospital, Fudan University.

All patients were evaluated firstly by history taking and pelvic examination (trimanual examination and digital rectal examination) by an experienced gynecologist (XSL) and then by examination with TVUS using "sliding signs" and, in 24 cases (80%), MRI. Patients who had been detected by TVUS or MRI to have the deep lesion and those whose did not but were highly suspected with DE by symptoms and pelvic examination were all arranged to undergo TVESG evaluation before surgery. A shear-wave TVESG (Supersonic Aixplorer Multiwave, Supersonic Imagine, Aix-en-Provence, France) was performed for all patients before surgery to measure the lesional stiffness of deep nodules. For all 30 patients recruited to this study, only two senior experienced ultrasound physicians were involved in doing both TVUS and TVESG. For TVESG evaluation, they performed B-mode TVUS before shifting to elastography mode to evaluate tissue stiffness in regions of interest (ROI).

The size of DE lesion was measured by ultrasound. During TVESG examination, a ROI was set in the typical lesional area of the deep nodule, and its stiffness value, in kilo Pascals or kPa, for the designated ROI was measured thrice, and the mean value was used. If the patient had two DE lesions at different locations, their stiffness values were measured and recorded for both lesions. In some cases, the stiffness values of the uterine corpus or the cervix were also measured in order to obtain a contrast between different tissues.

Among the recruited DE patients, 2 had two different sites of the deep lesions, and 2 patients had two different types of lesions (cystic and fibrotic). All DE lesions were detected by TVESG and were confirmed during operation. All lesional tissue samples were collected during operation, yielding 34 lesion samples in total. They were fixed with 10% formalin and paraffin-embedded for analyses.

For all patients, their demographic and clinical information was collected and recorded. This included age, gravidity,

parity, length of menstrual cycles, date of the last menstruation, the date of surgery, verbal descriptor rating (none, mild, moderate, and severe) and visual analog scale (VAS) on dysmenorrhea, site of lesions, rASRM scores and staging during surgery, and pathological reports.

### Immunohistochemistry and Masson Trichrome Staining

Serial 4-mm sections were made from each tissue block, with the first resultant slide stained for hematoxylin and eosin (H&E) to confirm the pathologic diagnosis.

Immunohistochemistry staining of E-cadherin, α smooth muscle actin, estrogen receptor β (ERβ), PR, CD31, and von Willebrand Factor (vWF) was performed for all DE tissue samples. Routine deparaffinization and rehydration procedures were performed. For antigen retrieval, the slides were heated at 98 °C in a citric acid buffer (pH 6.0) for a total of 30 min and cooled naturally to room temperature. Sections were then incubated with the E-cadherin primary antibody (1:400; CST, MA, USA), α-SMA (1:100; Abcam, Cambridge, England), ERβ (1:50; Abcam), PR (1:100; Abcam), CD31 (1:200; Abcam), or vWF (1:500; Abcam) overnight at 4 °C. After slides were rinsed, the horse radish peroxidase (HRP)-labeled secondary anti-rabbit/mouse antibody detection reagent (Shanghai Sun BioTech Company) was incubated for 30 min at room temperature. The bound antibody complexes were stained for about 1–2 min or until appropriate for microscopic examination with diaminobenzidine and then counterstained with hematoxylin (30 s) and mounted.

The positive staining was evaluated using a semiquantitative scoring system, as reported previously [41]. Briefly, the number and intensity of positive cells were counted using Image-Pro Plus 6.0 (Media Cybernetics Inc., Bethesda, MD, USA). A series of 3 to 5 randomly selected images on several sections were taken under X400 microscopic magnification to obtain a mean value. Immunohistochemical parameters assessed in the area detected included (a) integrated optical density (IOD); (b) total stained area (S); and (c) mean optical density (MOD), which is defined as MOD = IOD/S, equivalent to the intensity of stain in all positive cells [36]. CD31-labeled microvessel density (MVD) was counted under X200 microscopic magnification. Human invasive breast cancer, uterine fibroids, and adenomyosis tissue samples were used as positive controls. For negative controls, OE tissue samples were incubated with rabbit or mouse serum instead of primary antibodies (Supplementary Fig. S1).

Masson trichrome staining was used to detect collagen fibers in tissue samples and to quantify the extent of lesional fibrosis as previously reported [42]. The detailed description of the procedure can be found in the Supplementary Information.

### Statistical Analysis

The comparison of distributions of continuous variables between or among two or more groups was made using the Wilcoxon and Kruskal tests, respectively. Pearson's or Spearman's rank correlation coefficient was used when evaluating correlations between two variables when both variables were continuous or when at least one variable was ordinal. To evaluate which factors were associated with the tissue stiffness, multiple linear regression analysis was used. Jonckheere-Terpstra test was used to see whether there is trend among different severity groups.

$P$ values of $< 0.05$ were considered statistically significant. All computations were made with R version 3.5.1 (www.r-project.org).

## Results

The characteristics of patients recruited for this study are listed in Table 1. Multiple linear regression analysis incorporating age, parity, the co-occurrence with OE, adenomyosis, and/or uterine fibroids indicated that age and the presence of adenomyosis and/or uterine fibroids are positively associated with the uterine size (all 3 p's $< 0.019$, $R^2 = 0.60$).

The pelvic examination failed to detect 5 cases of DE, and among them, 2 lesions were at the pouch of Douglas (sizes = 1.0 and 2.0 cm, respectively), 1 each on the sacral ligament (size = 2 cm), bladder (lesion size = 1.8 cm), and the ureter (lesion size = 2.5 cm), yielding a total detection rate of 83.3%. The mean lesion size of the 5 cases missed by pelvic exam was significantly smaller than the 25 cases that were detected ($1.86 \pm 0.55$ cm versus $3.11 \pm 1.15$; $p = 0.015$; Fig. 1A). TVUS detected 20 (66.7%) cases out of 30. Among 24 of them who also received MRI examination, 20 (83.3%) were detected to have DE lesions. Similar to the pelvic examination, larger DE lesions were more likely to be detected by TVUS ($p = 0.0003$; Fig. 1B) and MRI ($p = 0.036$; Fig. 1C). Yet all DE cases that could not be diagnosed by TVUS or MRI were correctly diagnosed by TVESG. Irrespective of detection method or their combination, the DE lesions that evaded the detection were those small ones (Fig. 1A–C; Supplementary Fig. S2A).

Overall, TVESG provided a clear view of lesional stiffness and gave absolute stiffness values in kPa. For the 34 tissue samples, the mean lesional stiffness ranged from 40.9 to 295.1 kPa, averaging 134.7 kPa, with a median of 123.0 kPa. To be more inclusive and perhaps also more objective, we used all 34 DE lesions from the 30 patients whenever possible. There was no apparent relationship between the location of DE lesions and their stiffness, in part due to the small sample sizes in certain location categories. No relationship between the lesion size and lesional stiffness was found

**Table 1** Characteristics of recruited patients with deep endometriosis for this study

| Variable | Patient characteristics ($n = 30$) |
|---|---|
| Age (in years) | Mean = 38.2 (SD = 6.1)<br>Median = 38.5 range = 23–47 |
| Menstrual phase | |
| *Proliferative* | 11 (36.7%) |
| *Secretory* | 19 (63.3%) |
| Parity | |
| *0* | 5 (16.7%) |
| *1* | 21 (70.0%) |
| *≥2* | 4 (13.3%) |
| Severity of dysmenorrhea (VDR) | |
| *None* | 0 (0.0%) |
| *Mild* | 8 (26.7%) |
| *Moderate* | 8 (26.7%) |
| *Severe* | 14 (46.7%) |
| Scores of visual analog scale (VAS) on dysmenorrhea | Mean = 6.3 (SD = 3.4)<br>Median = 7 range = 3–9 |
| Comorbidity | |
| *None* | 6 (20.0%) |
| *Ovarian endometrioma* | 8 (26.7%) |
| *Adenomyosis* | 4 (13.3%) |
| *Ovarian endometrioma & adenomyosis* | 12 (40.0%) |
| Sites of the lesions | |
| *Pouch of Douglas* | 12 (40%) |
| *Sacral ligament* | 3 (10%) |
| *Rectovaginal* | 10 (33.3%) |
| *Rectovaginal and vaginal fornix* | 1 (3.3%) |
| *Pouch of Douglas and vaginal fornix* | 1 (3.3%) |
| *Ureter* | 2 (6.7%) |
| *Bladder* | 1 (3.3%) |
| rASRM staging | |
| *I (score 1–5)* | 0 (0.0%) |
| *II (score 6–15)* | 1 (3.3%) |
| *III (score 16–40)* | 2 (6.7%) |
| *IV (score > 40)* | 27 (90%) |
| Co-occurrence of uterine fibroids | |
| *No* | 16 (53.3%) |
| *Yes* | 14 (46.7%) |
| Uterine size ($cm^3$) | Mean = 91.8 (S.D. = 53.5)<br>Median = 73.5, range = 20.6–223.7<br>(1 case missing, due to previous subtotal hysterectomy) |

Abbreviations used: *rASRM* Revised American Society of Reproductive Medicine Classification system; *SD* standard deviation; *VDR* verbal descriptor rating

(r = − 0.06, $p = 0.87$). The severity of dysmenorrhea was not correlated with lesional stiffness nor with the lesion size (Spearman's r ranged from 0.05 to 0.20, all p's > 0.26). However, the severity of dysmenorrhea was associated with the uterine size (Spearman's r = 0.42, $p = 0.022$ for VDR, and r = 0.41, $p = 0.026$ for VAS, respectively).

While the difference in lesional stiffness between DE cases who were missed and detected by pelvic examination, TVUS or MRI did not reach statistical significance (all p's > 0.14; Fig. 1D-F), it is likely due to the lack of statistical power as the number of DE cases that were missed by pelvic examination, TVUS, or MRI were 5, 10, and 4, respectively. Indeed, their lesional stiffness appeared to be higher than those that were detected, although the difference did not reach statistical significance (Fig. 1D-F). In fact, regardless of the detection method or their combinations, the DE lesions that evaded the detection on average had higher stiffness than those that did not (Supplementary Fig. S2B). Since all of them were detected by TVESG, this seems to suggest that the use of information on lesional stiffness helped TVESG to make the correct diagnosis.

We arbitrarily set a cut-off of 100 kPa and divided 34 samples into the low or high lesional stiffness group depending on the lesional stiffness < or ≧ 100 kPa. For the low-stiffness group, the lesional stiffness ranged from 40.9 to 98.2 kPa, with a median of 66.1 kPa. In contrast, it ranged from 105.4 to 295.1 kPa, with a median of 156.5 kPa, in the high-stiffness group. Among the 34 lesion samples, 4 (11.8%), 7 (20.6%), and 12 (35.3%) of them had stiffness values less than 50 kPa, 80 kPa, and 100 kPa, respectively, suggesting that there is a sizable portion of DE lesions are "soft" or still not progressed to "old" lesions.

We next evaluated the relationship, if any, between the lesional stiffness and the extent of lesional fibrosis and the lesional expression levels of E-cadherin (a marker of EMT, scored in the epithelial component only), α-SMA (a marker for FMT, scored in the stromal component only), and hormonal receptors ERβ and PR and also the CD31-positive MVD and the density of more mature blood vessels (vWF-positive) in DE lesions.

We found that E-cadherin staining was seen in glandular epithelial cells of the ectopic endometrium and was localized in the cell membrane. α-SMA staining was seen primarily in the stroma of lesions. ERβ staining was seen mostly in glandular epithelial cells and stromal cells as well of the ectopic endometrium and was localized in the nuclei and cytoplasm. PR staining was seen in the nuclei of both stromal and glandular epithelial cells of the ectopic endometrium (Fig. 2). Consistent with what have been reported, most DE lesions exhibited extensive fibromuscular content (Fig. 3). We contrast the immunohistochemistry and histochemistry results in lesions with low and high lesional stiffness in Figs. 2 and 3, which show striking difference between the two groups.

We found that there was a highly statistically significant difference in lesional staining of E-cadherin, α-SMA, ERβ, and PR, as well as the extent of fibrosis, MVD and vascular density between the low- and high-stiffness groups (all p's < 0.0002; Fig. 4).

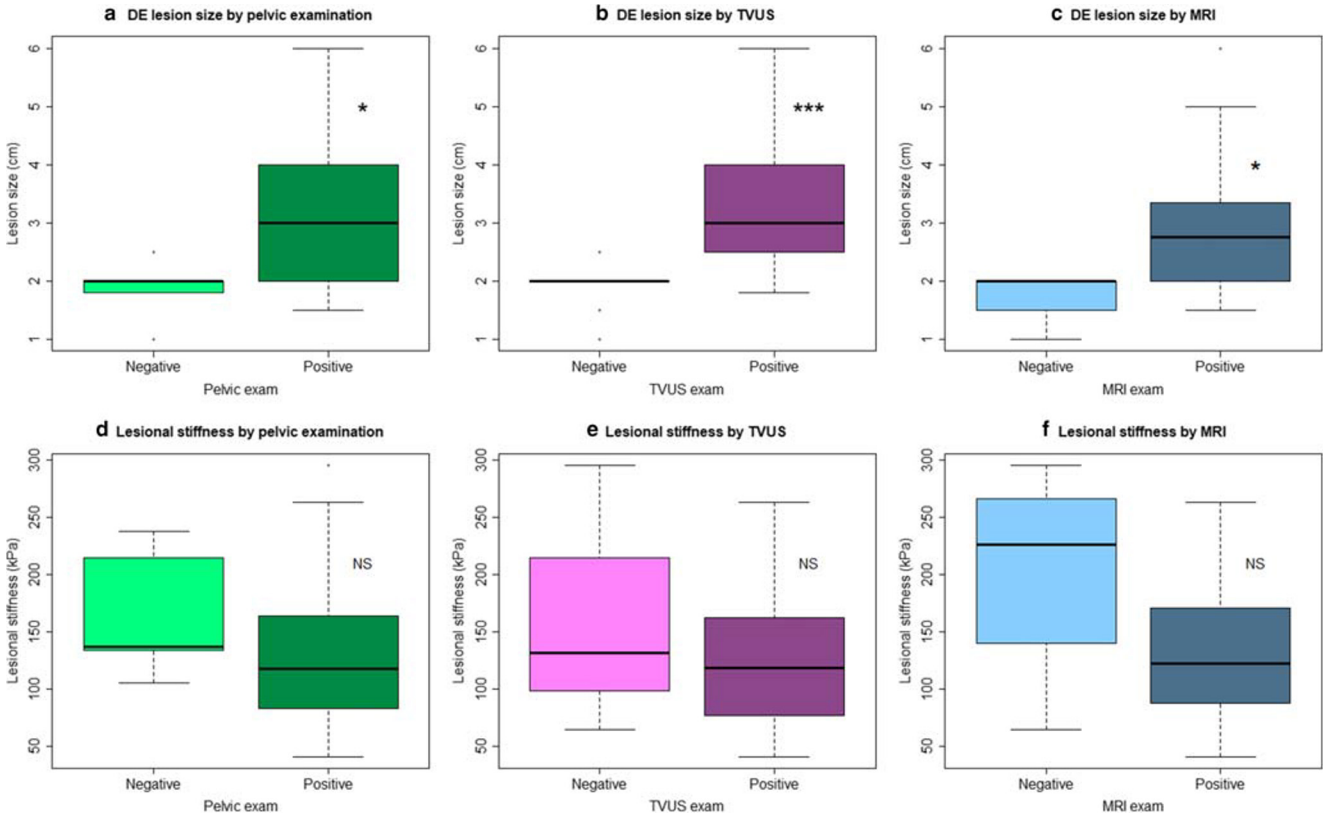


**Fig. 1** Boxplots showing the size and stiffness of lesions that were positively identified or missed by different detection methods. Lesion size by positive or negative identification by pelvic examination (**A**), TVUS (**B**) and MRI (**C**). Lesional stiffness per TVESG by positivity of pelvic examination (**D**), TVUS (**E**), and MRI (**F**). Symbols of statistical significance: *: $p < 0.05$; ***: $p < 0.001$; NS: $p > 0.05$

Given the divergent staining patterns between the low- and high-stiffness groups, we next tried to find the relationship, if any, between lesional stiffness and lesional histology. We found that the mean lesional stiffness correlated closely with the extent of lesional fibrosis, as determined by the Masson trichrome staining ($r = 0.89$, $p = 3.4 \times 10^{-12}$; Fig. 5A). It also correlated negatively with the staining levels of E-cadherin and of PR ($r = -0.91$, $p = 7.0 \times 10^{-14}$, and $r = -0.92$, $p = 7.6 \times 10^{-15}$, respectively; Fig. 5B,E), but positively with the staining levels of α-SMA and of ERβ ($r = 0.84$, $p = 4.9 \times 10^{-10}$, and $r = 0.89$, $p = 3.3 \times 10^{-12}$, respectively; Fig. 5C,D).

Since the ratio of the extent of fibrosis versus the PR expression levels may indicate how responsive the lesion would be to hormonal treatment, we also plotted the lesional stiffness against the ratio and found that the two variables were highly correlated ($r = 0.93$, $p = 1.2 \times 10^{-15}$; Fig. 5F). The mean lesional stiffness also correlated negatively with lesional MVD as well as the vascular density ($r = -0.89$, $p = 2.1 \times 10^{-12}$, and $r = -0.91$, $p = 1.5 \times 10^{-13}$, respectively; Fig. 5G, H). Using the maximum lesional stiffness instead of the mean lesional stiffness yielded nearly identical results (data not shown).

Multiple linear regression incorporating age, parity, menstrual phase, co-occurrence with OE, uterine fibroids, and/or adenomyosis, lesion size, extent of lesional fibrosis, ERβ staining levels, MVD, and vWF-positive vascularity as co-variables indicated that the extent of lesional fibrosis and ERβ staining levels were positively, while the lesional vascularity and being the rectovaginal location were negatively, associated with the lesional stiffness (all $p$ values<0.023, $R^2 = 0.91$). That is, age, parity, lesion size, and the co-occurrence of OE, adenomyosis, and/or fibroids did not significantly influence the lesional stiffness, but the extent of lesional fibrosis and lesional ERβ staining levels were positively, while the lesional vascularity and being the rectovaginal location were negatively, associated with the lesional stiffness.

Within DE lesions, the extent of fibrosis correlated negatively with the E-cadherin and PR staining levels ($r = -0.84$, $p = 5.1 \times 10^{-10}$, and $r = -0.81$, $p = 9.5 \times 10^{-9}$, respectively; Fig. 6A, D) but positively with staining levels of α-SMA and of ERβ ($r = 0.91$, $p = 2.0 \times 10^{-13}$, $r = 0.82$, $p = 2.2 \times 10^{-9}$, respectively; Fig. 6B, C). It also correlated negatively with lesional MVD as well as the vascular density ($r = -0.83$, $p = 8.5 \times 10^{-10}$, and $r = -0.72$, $p = 1.4 \times 10^{-6}$, respectively; Fig. 6E, F), indicating that the lesional vascularity decreases as DE lesions become more fibrotic, or vice versa. These results also indicate that the extent of lesional fibrosis is a function of the completeness and thoroughness of the EMT and FMT, a finding we reported previously [40].

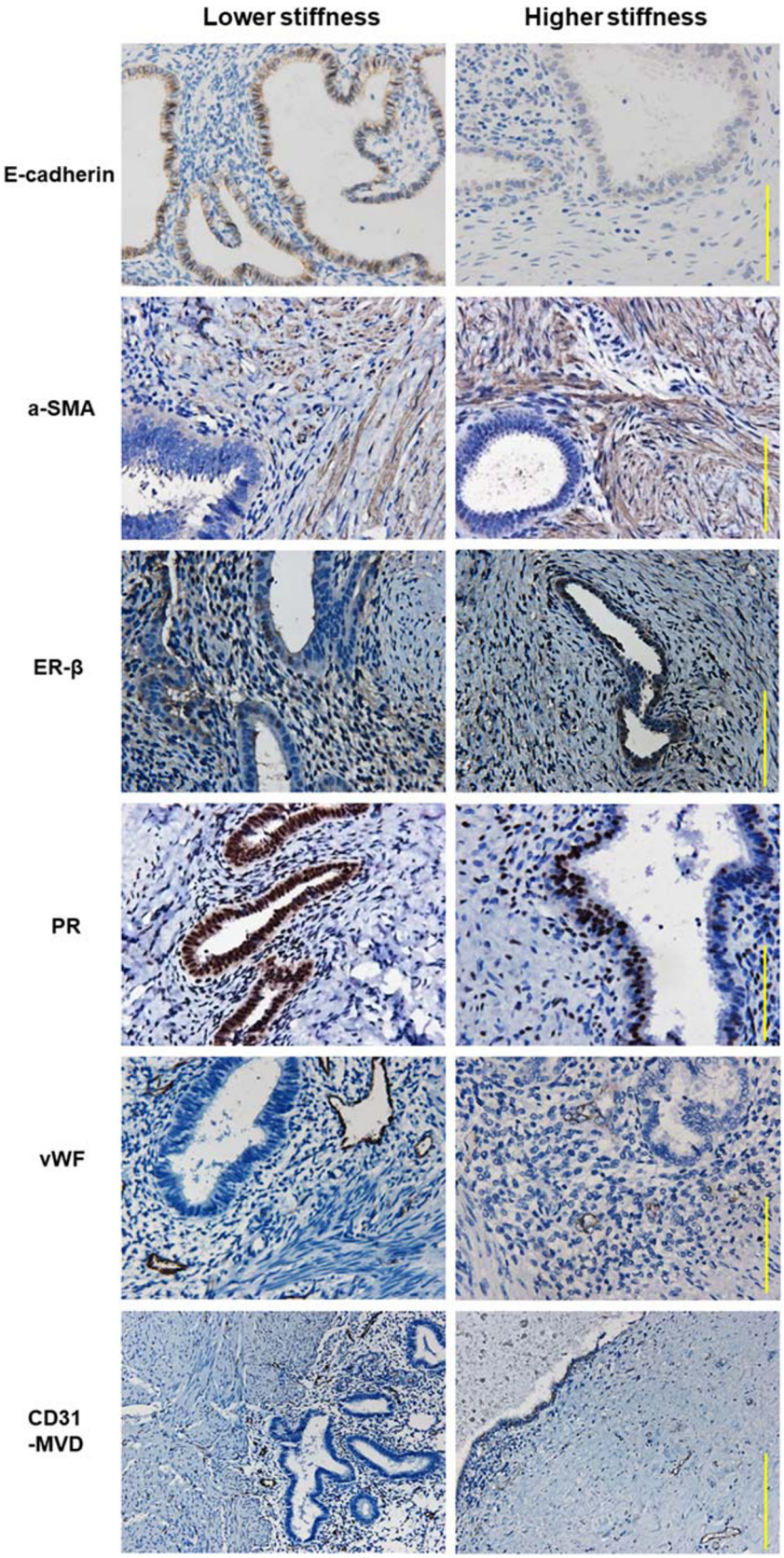


**Fig. 2** Representative immunoreactivity staining of E-cadherin, α-SMA, ERβ, PR, vWF, and CD31-MVD in DE lesions from lower stiffness and higher stiffness lesions. Left column, lower stiffness lesion (mean stiffness value = 62.2 kPa); right column, higher stiffness lesion (mean stiffness value = 262.7 kPa). Magnification in all figures except CD31-MVD: X400. The scale bar represents 125 μm. Magnification in CD31-MVD figures: X200. The scale bar represents 251 μm

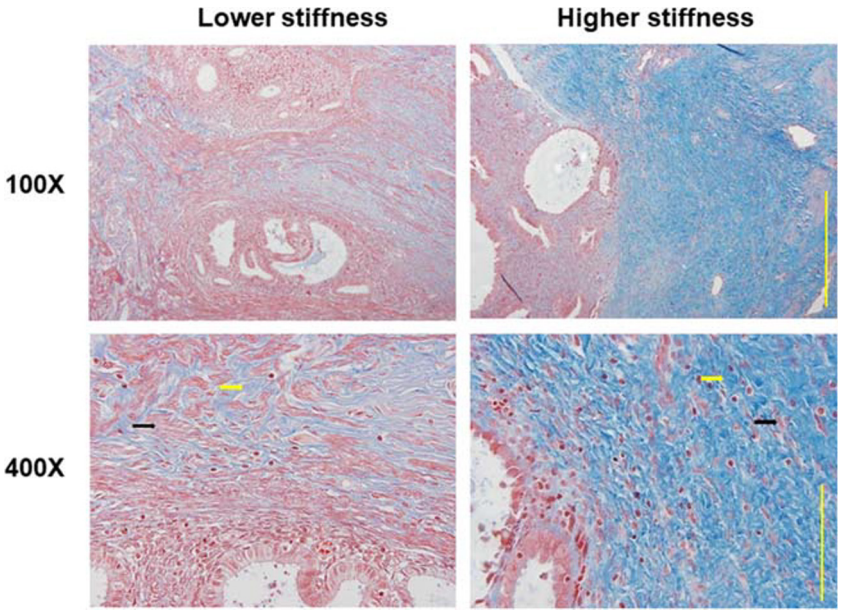


**Fig. 3** Representative Masson staining in DE lesions from lower stiffness (mean stiffness value = 62.2 kPa) and higher stiffness lesions (mean stiffness value = 262.7). Magnification in figures of left column: X100. The scale bar represents 502 μm. Magnification in figures of right column: X400. The scale bar represents 125 μm. Yellow arrows point to collagen fibers stained in blue, while black arrows indicate muscle fibers stained in red

The mean lesional stiffness did not seem to correlate with the severity of dysmenorrhea (r = 0.10, $p = 0.59$ and r = 0.22, $p = 0.23$, for VDR and VAS, respectively).

Multiple linear regression incorporating age, parity, menstrual phase, co-occurrence with OE, uterine fibroids, and/or adenomyosis, lesion size, uterine size, mean lesional stiffness, and location of lesions as co-variables indicated that the co-occurrence with adenomyosis was the only variable that was positively associated with the VAS scores ($p = 0.0029$, $R^2 = 0.28$), indicating that aside from the co-occurrence with adenomyosis, there are other factors, yet to be identified, that determine the severity of dysmenorrhea.

## Discussion

In the last decade, ESG has emerged as a novel imaging technique for noninvasive assessment of tissue mechanical

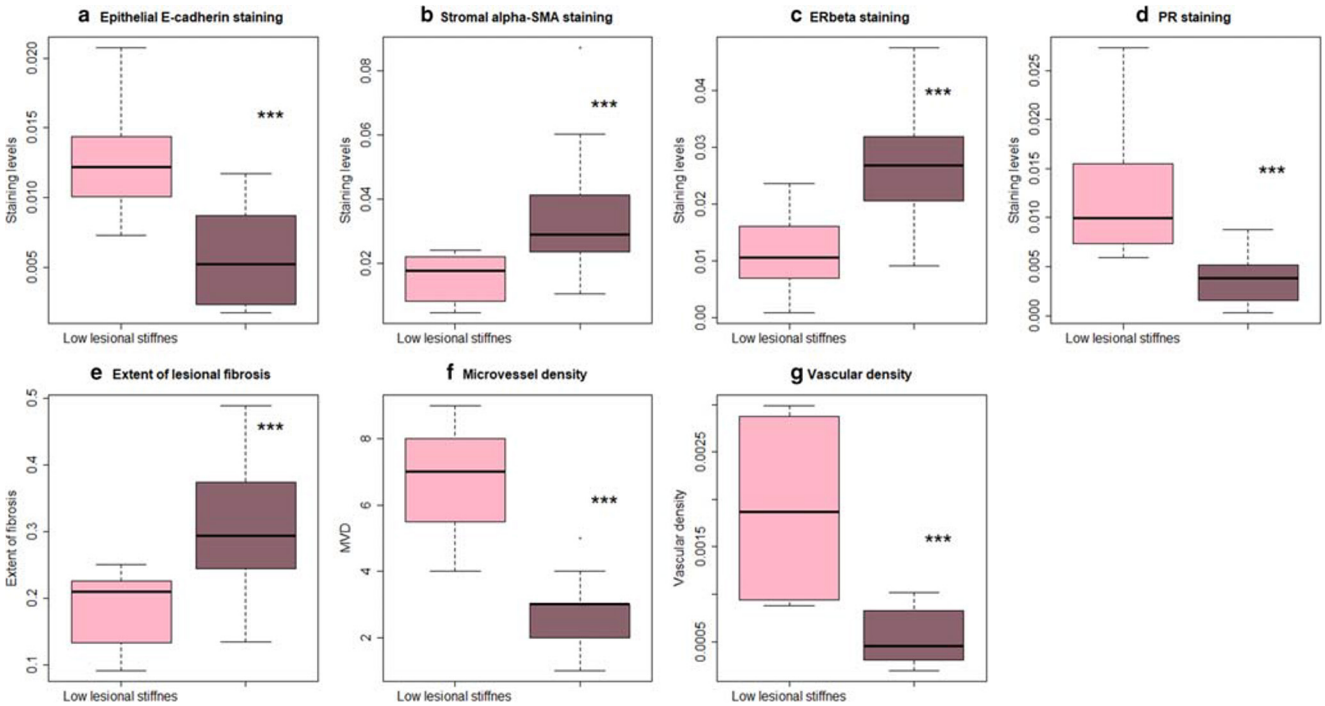


**Fig. 4** Boxplots showing the difference in lesional immunostaining and histostaining levels between low- and high-stiffness groups. (**A**) epithelial E-cadherin staining; (**B**) stromal α-SMA staining; (**C**) ERβ staining; (**D**) PR staining; (**E**) Extent of lesional fibrosis; (**F**) CD31-MVD; and (**G**) vWF-positive vascular density. Symbol for the statistical significance level: ***: $p < 0.001$

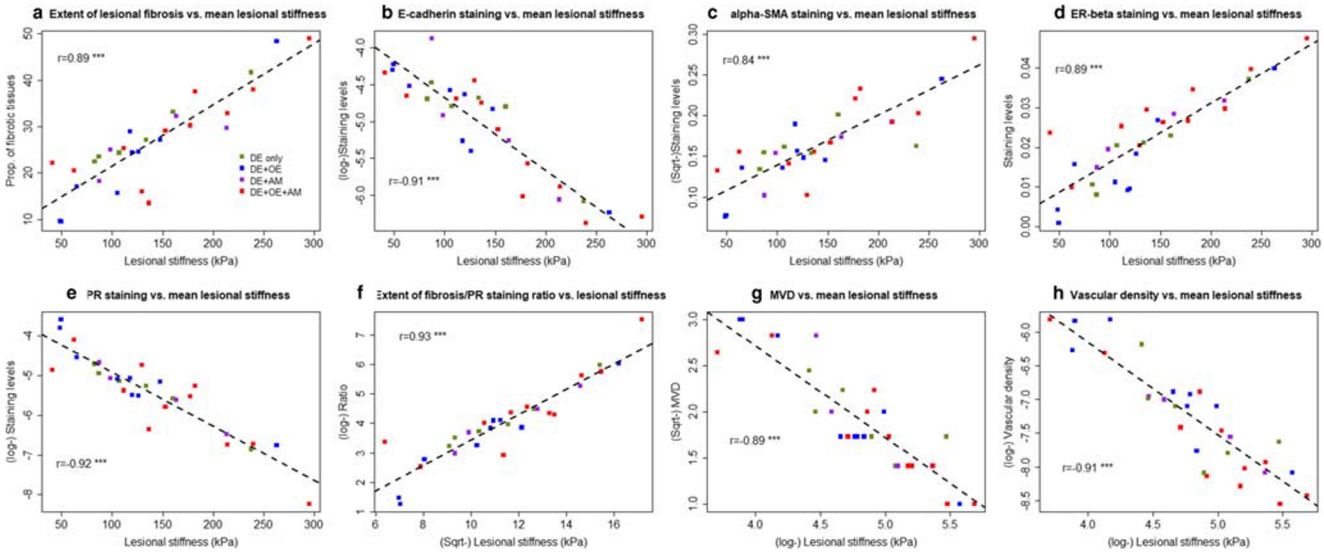


**Fig. 5** Scatter plot of lesional stiffness versus (**A**) the extent of lesional fibrosis; (**B**) E-cadherin staining levels; (**C**) α-SMA staining levels; (**D**) ERβ staining levels; (**E**) progesterone receptor staining levels; (**F**) the extent of fibrosis vs. PR expression ratio; (**G**) microvessel density (MVD), and (**H**) density of vWF-positive blood vessels in patients with deep endometriosis. The dashed line represents the regression line. The number shown is the correlation coefficient, along with the symbol showing the levels of statistical significance. ***: $p < 0.001$. The color of the dots in the figure indicates whether the patient has deep endometriosis (DE) alone (olive drab), DE and ovarian endometrioma (OE) (blue), DE and adenomyosis (AM) (purple), and DE with co-occurrence of OE and AM (red)

properties such as stiffness [43]. This technique capitalizes on the aberrant tissue elasticity embedded in various pathological organs or tissues to extract qualitative and quantitative information for diagnostic purposes. Dubbed as a "palpation imaging," ESG has been used successfully in characterizing breast tumor and staging and hepatic fibrosis [27, 28, 43]. Whenever palpation is of clinical values as in clinical examination in suspected DE cases [44], ESG should be of use [27]. As more and more manufacturers now incorporate ESG features into conventional ultrasonography, TVESG are becoming more available, affordable, and ease of use just like conventional TVUS.

The fibrogenesis in endometriotic and adenomyotic lesions is now well appreciated [45–48] and in fact a proposal has been made recently to redefine endometriosis to incorporate its fibrotic nature [49]. As the hallmark of fibrosis is the accumulation of collagen fibers, which results in increased tissue stiffness, TVESG is well-suited for diagnosing DE and adenomyosis since fibrosis and tissue stiffness are intricately coupled, as we have shown here and previously [36]. This is of particular importance since DE has been shown to be closely linked with focal adenomyosis [50, 51] and since TVESG can be easily employed to look for DE and adenomyosis in just one single examination. In addition, the "sliding sign" technique often used in TVUS to assess the mobility of uterus or bladder [52] is essentially the result of the absence or presence of adhesion. Yet adhesion itself also results from tissue fibrosis and could potentially be detected with ESG. Thus, TVESG not only has all the features of a conventional TVUS but also it can detect and exploit the differential stiffness between DE lesions and their surrounding tissues, thus potentially enhances its diagnostic accuracy.

As shown in Fig. 1 and Supplementary Fig. S2, DE lesions that evaded the detection by either pelvic examination, TVUS, MRI or their combinations tend to be much smaller than those did not, but nonetheless they were all detected by TVESG since they had higher stiffness. In other words, by use of additional information on differential stiffness between lesions and their surrounding tissues, TVESG was able to detect those DE lesions that were small yet had higher stiffness. Without the stiffness information, the small lesions seen under TVUS (and, to certain extent, MRI) examination may look like adhesion of ovarian endometriomas with the lower and posterior part of the uterus, or the adhesion of the lower and posterior part of the uterus with the pouch of Douglas or bowels, and consequently miss the diagnosis.

Our findings that lesional stiffness correlated closely with lesional fibrosis suggests that the TVESG can tell us roughly the developmental stage of the DE lesions. In addition, the correlation between lesional stiffness and hormonal receptor expression, the EMT and FMT marker expression, and the vascularity in DE lesions strongly suggests that TVESG not only can provide an instant assessment of the developmental stage of DE lesions but also may be employed to help physicians to choose the best treatment modality for the patient.

Indeed, DE is notoriously challenging for medical treatment [53, 54], and the precise underlying causes are largely unclear. For a DE lesion that is highly fibrotic as manifested by the high stiffness reading under TVESG, its response to hormonal treatment is likely to be poor due to concomitant low PR expression as well as reduced vascularity, since any drug that is

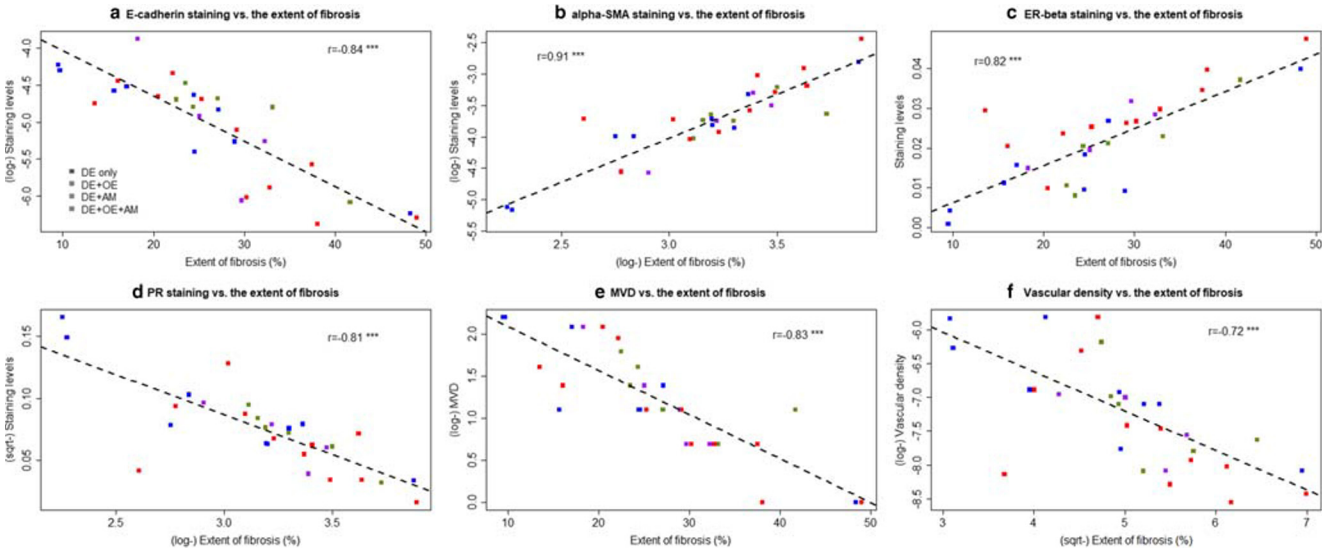


**Fig. 6** Scatter plot of the lesional fibrosis versus (**A**) E-cadherin staining levels; (**B**) α-SMA staining levels; (**C**) ERβ staining levels; (**D**) progesterone receptor staining levels; (**F**) microvessel density (MVD), and (**G**) density of vWF-positive blood vessels in patients with deep endometriosis. The dashed line represents the regression line. The number shown is the correlation coefficient, along with the symbol showing the levels of statistical significance. ***: $p < 0.001$. The color of the dots in the figure indicates whether the patient has deep endometriosis (DE) alone (olive drab), DE and ovarian endometrioma (OE) (blue), DE and adenomyosis (AM) (purple), and DE with co-occurrence of OE and AM (red)

administrated systemically or even locally would be difficult to reach the target tissues that are DE lesions and, for hormonal drugs, difficult to elicit response to progesterone. On the other hand, we can see that there is a sizable portion of DE lesions that have lower lesional stiffness and have not progressed to highly fibrotic stage, suggesting that they might be responsive to hormonal treatment and thus can avoid surgery. Of course, future studies are needed to demonstrate this is the case empirically.

Our results are consistent with our previous report that, compared to OE, DE lesions underwent more thorough and extensive EMT, FMT, and SMM and, consequently, displayed significantly higher fibrotic content but less vascularity [40]. As we have shown recently, this difference is attributable to the difference in the microenvironment between OE and DE lesions, and in particular sensory nerve-derived neuropeptides play an important role in facilitating the lesional development and in shaping the lesional destiny [19, 55]. Thus, our study further corroborates the notion that endometriotic lesions are essentially wounds undergoing ReTIAR [39]. In addition, through demonstration of the potential of TVESG in diagnosing DE, our study illustrates that better understanding of the pathophysiology could yield better diagnostic procedures and perhaps better therapeutics in the future.

Our finding that the lesional stiffness as measured by TVESG correlated closely with the extent of fibrosis (Fig. 5A) is remarkably similar to our previous use of TVESG to diagnose adenomyosis [36], even though two different types of elastography instruments were used. This is also consistent with the close correlation between the renal cortical stiffness and histological fibrosis determinants in patients with kidney transplantation [56]. This close correlation suggests that the TVESG can tell us roughly the developmental stage of the DE lesions. In addition, the correlation between lesional stiffness and hormonal receptor expression, the EMT and FMT marker expression, and the vascularity in DE lesions strongly suggests that TVESG not only can provide an instant assessment of the developmental stage of DE lesions but also may be employed to help physicians to choose the best treatment modality for the patient.

While it is entirely biologically plausible that DE lesions with low stiffness may respond well to hormonal treatment yet those with high stiffness may not, empirical data are still needed to test this hypothesis. In addition, when both DE and adenomyosis co-occur, as is often the case for focal adenomyosis [50, 51], whether the information on DE lesional stiffness in conjunction with on adenomyotic lesions would account for the variation in the severity of dysmenorrhea or of other pains would require future clarification.

By the combined use of TVESG and the histological analysis of DE lesions based on their known natural history, this study has the strength of linking lesional stiffness with the histological changes in the lesions. By establishing the close correlation between lesional stiffness and the extent of fibrosis, this study essentially demonstrates the potential of TVESG in diagnosing DE. In addition, by establishing a relationship between lesional stiffness and hormonal receptor expression and vascularity in lesions, our study provides a tantalizing and exciting possibility that the findings from TVESG could help choose the best

treatment modality for the patient. Moreover, by showing the lesional features that the existing diagnostic procedures failed to detect while TVESG successfully picked up, our study clearly demonstrates the great potential that TVESG has in improving the diagnostic accuracy for DE.

There are several limitations in this study. First, while slightly over half of our recruited DE patients also had adenomyosis which appeared to account for the severity of dysmenorrhea, we did not measure the stiffness of adenomyotic lesions. This omission, clearly an oversight on our part, may be responsible for our failure to find any clear relationship between DE lesional stiffness and the severity of dysmenorrhea. In future studies, the stiffness of adenomyotic lesions also should be measured by TVESG and incorporated into the analysis in the setting of DE. Given our finding that the severity of dysmenorrhea is associated with the uterus size, which, in turn, is associated with the co-occurrence of adenomyosis, it is likely that the histology of adenomyosis may account for a sizable portion of variation in dysmenorrhea severity even in the presence of DE.

Second, due to the design of this study, we did not specifically estimate the sensitivity and specificity of diagnosing DE using TVESG, even though the sensitivity was 100%. Along the similar vein, we did not evaluate the inter-observer agreement when determining lesional stiffness, which also is important for a diagnostic procedure. This is mainly due to our initial intention to demonstrate the utility of using TVESG to diagnose DE, in particular, to demonstrate the relationship between measured lesional stiffness and the extent of lesional fibrosis. Future studies are needed to estimate the sensitivity, specificity, and perhaps other characteristics for TVESG.

In summary, TVESG has a great potential in diagnosing DE since it uses additional information on the differential stiffness between DE lesions and their surrounding tissues. It not only can provide an instant—albeit rough—assessment of the developmental stage of DE lesions but also may be used to guide the choice of the best treatment modality for the patient.

**Acknowledgments** The authors would like to thank Dr. Cai Chang and Na Hu from Shanghai Tumor Hospital, Fudan University, and Dr. Li Sun from Shanghai OB/GYN Hospital, Fudan University, for their expert assistance in the TVESG examination for the recruited DE patients. We thank an anonymous reviewer for his/her constructive comments and suggestions on an earlier version of this manuscript.

## Compliance with Ethical Standards

**Conflict of Interest** The authors declare that they have no conflicts of interest.

**Grant support** This research was supported in part by grants 81530040 (SWG), 81771553 (SWG), and 81671436 (XSL) from the National Natural Science Foundation of China, and a grant from Ningbo Municipal Bureau of Science and Technology (2017A610169).

## References

1. Nisolle M, Donnez J. Peritoneal endometriosis, ovarian endometriosis, and adenomyotic nodules of the rectovaginal septum are three different entities. Fertil Steril. 1997;68:585–96.
2. Koninckx PR. Biases in the endometriosis literature. Illustrated by 20 years of endometriosis research in Leuven. Eur J Obstet Gynecol Reprod Biol. 1998;81:259–71.
3. Koninckx PR, Ussia A, Adamyan L, Wattiez A, Donnez J. Deep endometriosis: definition, diagnosis, and treatment. Fertil Steril. 2012;98:564–71.
4. Tosti C, Pinzauti S, Santulli P, Chapron C, Petraglia F. Pathogenetic Mechanisms of Deep Infiltrating Endometriosis. Reprod Sci. 2015.
5. Ballester M, Belghiti J, Zilberman S, Thomin A, Bonneau C, Bazot M, et al. Surgical and clinical impact of extraserosal pelvic fascia removal in segmental colorectal resection for endometriosis. J Minim Invasive Gynecol. 21:1041–8.
6. Van den Bosch T, Van Schoubroeck D. Ultrasound diagnosis of endometriosis and adenomyosis: state of the art. Best Pract Res Clin Obstet Gynaecol. 2018;51:16–24.
7. Bazot M, Bornier C, Dubernard G, Roseau G, Cortez A, Darai E. Accuracy of magnetic resonance imaging and rectal endoscopic sonography for the prediction of location of deep pelvic endometriosis. Hum Reprod. 2007;22:1457–63.
8. Abrao MS, Goncalves MO, Ajossa S, Melis GB, Guerriero S. The sonographic diagnosis of deep endometriosis. J Ultrasound Med. 2009;28:408–9 author reply 9-10.
9. Guerriero S, Ajossa S, Minguez JA, Jurado M, Mais V, Melis GB, et al. Accuracy of transvaginal ultrasound for diagnosis of deep endometriosis in uterosacral ligaments, rectovaginal septum, vagina and bladder: systematic review and meta-analysis. Ultrasound Obstet Gynecol. 2015;46:534–45.
10. Guerriero S, Ajossa S, Orozco R, Perniciano M, Jurado M, Melis GB, et al. Accuracy of transvaginal ultrasound for diagnosis of deep endometriosis in the rectosigmoid: systematic review and meta-analysis. Ultrasound Obstet Gynecol. 2016;47:281–9.
11. Guerriero S, Saba L, Pascual MA, Ajossa S, Rodriguez I, Mais V, et al. Transvaginal ultrasound vs magnetic resonance imaging for diagnosing deep infiltrating endometriosis: systematic review and meta-analysis. Ultrasound Obstet Gynecol. 2017;51:586–95.
12. Nisenblat V, Bossuyt PM, Farquhar C, Johnson N, Hull ML. Imaging modalities for the non-invasive diagnosis of endometriosis. Cochrane Database Syst Rev. 2016;2:CD009591.
13. Hudelist G, English J, Thomas AE, Tinelli A, Singer CF, Keckstein J. Diagnostic accuracy of transvaginal ultrasound for non-invasive diagnosis of bowel endometriosis: systematic review and meta-analysis. Ultrasound Obstet Gynecol. 2011;37:257–63.
14. Exacoustos C, Malzoni M, Di Giovanni A, Lazzeri L, Tosti C, Petraglia F, et al. Ultrasound mapping system for the surgical management of deep infiltrating endometriosis. Fertil Steril. 2014;102:143–50 e2.
15. Bazot M, Darai E. Diagnosis of deep endometriosis: clinical examination, ultrasonography, magnetic resonance imaging, and other techniques. Fertil Steril. 2017;108:886–94.
16. Zhang Q, Duan J, Liu X, Guo SW. Platelets drive smooth muscle metaplasia and fibrogenesis in endometriosis through epithelial-mesenchymal transition and fibroblast-to-myofibroblast transdifferentiation. Mol Cell Endocrinol. 2016;428:1–16.
17. Duan J, Liu X, Guo S-W. The M2a macrophage subset may be critically involved in fibrogenesis of endometriosis in mouse. Reprod BioMed Online. 2018;37:254–68.
18. Benagiano G, Guo SW, Puttemans P, Gordts S, Brosens I. Progress in the diagnosis and management of adolescent endometriosis: an opinion. Reprod Biomed Online. 36:102–14.

19. Liu X, Yan D, Guo SW. Sensory nerve-derived neuropeptides accelerate the development and fibrogenesis of endometriosis. Hum Reprod. 2019;34:452–68.
20. Liu X, Zhang Q, Guo SW. Histological and Immunohistochemical characterization of the similarity and difference between ovarian Endometriomas and deep infiltrating endometriosis. Reprod Sci. 2017;25:329–40.
21. Yan D, Liu X, Guo SW. Neuropeptides substance P and calcitonin gene related peptide accelerate the development and Fibrogenesis of endometriosis. Sci Rep. 2019;9:2698.
22. Anaf V, Chapron C, El Nakadi I, De Moor V, Simonart T, Noel JC. Pain, mast cells, and nerves in peritoneal, ovarian, and deep infiltrating endometriosis. Fertil Steril. 2006;86:1336–43.
23. Anaf V, El Nakadi I, Simon P, Van de Stadt J, Fayt I, Simonart T, et al. Preferential infiltration of large bowel endometriosis along the nerves of the colon. Hum Reprod. 2004;19:996–1002.
24. Bazot M, Detchev R, Cortez A, Amouyal P, Uzan S, Darai E. Transvaginal sonography and rectal endoscopic sonography for the assessment of pelvic endometriosis: a preliminary comparison. Hum Reprod. 2003;18:1686–92.
25. Odagiri K, Konno R, Fujiwara H, Netsu S, Yang C, Suzuki M. Smooth muscle metaplasia and innervation in interstitium of endometriotic lesions related to pain. Fertil Steril. 2009;92:1525–31.
26. Shiina T, Nightingale KR, Palmeri ML, Hall TJ, Bamber JC, Barr RG, et al. WFUMB guidelines and recommendations for clinical use of ultrasound elastography: part 1: basic principles and terminology. Ultrasound Med Biol. 2015;41:1126–47.
27. Gennisson JL, Deffieux T, Fink M, Tanter M. Ultrasound elastography: principles and techniques. Diagn Interv Imaging. 2013;94:487–95.
28. Srinivasa Babu A, Wells ML, Teytelboym OM, Mackey JE, Miller FH, Yeh BM, et al. Elastography in chronic liver disease: modalities, techniques, limitations, and future directions. Radiographics. 2016;36:1987–2006.
29. Cosgrove D, Piscaglia F, Bamber J, Bojunga J, Correas JM, Gilja OH, et al. EFSUMB guidelines and recommendations on the clinical use of ultrasound elastography. Part 2: clinical applications. Ultraschall Med. 2013;34:238–53.
30. Mezzi G, Ferrari S, Arcidiacono PG, Di Puppo F, Candiani M, Testoni PA. Endoscopic rectal ultrasound and elastosonography are useful in flow chart for the diagnosis of deep pelvic endometriosis with rectal involvement. J Obstet Gynaecol Res. 2011;37:586–90.
31. Schiffmann ML, Schafer SD, Schuring AN, Kiesel L, Sauerland C, Gotte M, et al. Importance of transvaginal ultrasound applying elastography for identifying deep infiltrating endometriosis - a feasibility study. Ultraschall Med. 2014;35:561–5.
32. Fawzy M, Amer T. Efficacy of transabdominal sonoelastography in the diagnosis of caesarean section scar endometrioma: a pilot study. J Obstet Gynaecol. 2015;35:832–4.
33. Wozniak S, Czuczwar P, Szkodziak P, Wozniakowska E, Milart P, Paszkowski M, et al. Elastography improves the accuracy of ultrasound in the preoperative assessment of abdominal wall endometriosis. Ultraschall Med. 2015;36:623–9.
34. Batur A, Yavuz A, Ozgokce M, Bora A, Bulut MD, Arslan H, et al. The utility of ultrasound elastography in differentiation of endometriomas and hemorrhagic ovarian cysts. J Med Ultrason. 2016;43:395–400.
35. Herek D, Karabulut A, Agladioglu K. Usefulness of transabdominal real-time sonoelastography in the evaluation of ovarian lesions: preliminary results. Br J Radiol. 2016;89:20160173.
36. Liu X, Ding D, Ren Y, Guo SW. Transvaginal Elastosonography as an imaging technique for diagnosing Adenomyosis. Reprod Sci. 2018;25:498–514.
37. Liu X, Shen M, Qi Q, Zhang H, Guo SW. Corroborating evidence for platelet-induced epithelial-mesenchymal transition and fibroblast-to-myofibroblast transdifferentiation in the development of adenomyosis. Hum Reprod. 2016;31:734–49.
38. Shen M, Liu X, Zhang H, Guo SW. Transforming growth factor beta1 signaling coincides with epithelial-mesenchymal transition and fibroblast-to-myofibroblast transdifferentiation in the development of adenomyosis in mice. Hum Reprod. 2016;31:355–69.
39. Guo SW. Fibrogenesis resulting from cyclic bleeding: the holy grail of the natural history of ectopic endometrium. Hum Reprod. 2018.
40. Liu X, Zhang Q, Guo SW. Histological and Immunohistochemical characterization of the similarity and difference between ovarian Endometriomas and deep infiltrating endometriosis. Reprod Sci. 2018;25:329–40.
41. Ding D, Cai X, Zheng H, Guo SW, Liu X. Scutellarin suppresses platelet aggregation and stalls Lesional progression in mouse with induced endometriosis. Reprod Sci. 2018;1933719118817661.
42. Zhang Q, Duan J, Olson M, Fazleabas A, Guo SW. Cellular changes consistent with epithelial-Mesenchymal transition and fibroblast-to-Myofibroblast Transdifferentiation in the progression of experimental endometriosis in baboons. Reprod Sci. 2016;23:1409–21.
43. Sigrist RMS, Liau J, Kaffas AE, Chammas MC, Willmann JK. Ultrasound Elastography: review of techniques and clinical applications. Theranostics. 2017;7:1303–29.
44. Abrao MS, Goncalves MO, Dias JA Jr, Podgaec S, Chamie LP, Blasbalg R. Comparison between clinical examination, transvaginal sonography and magnetic resonance imaging for the diagnosis of deep endometriosis. Hum Reprod. 2007;22:3092–7.
45. Zhang Q, Duan J, Liu X, Guo SW. Platelets drive smooth muscle metaplasia and fibrogenesis in endometriosis through epithelial-mesenchymal transition and fibroblast-to-myofibroblast transdifferentiation. Mol Cell Endocrinol 2016;In press. .
46. Zhang Q, Liu X, Guo SW. Progressive development of endometriosis and its hindrance by anti-platelet treatment in mice with induced endometriosis. Reprod BioMed Online. 2017;34:124–36.
47. Liu X, Shen S, Qi Q, Zhang H, Guo S-W. Corroborating evidence for platelet-induced epithelial-Mesenchymal transition and fibroblast-to-Myofibroblast Transdifferentiation in the development of Adenomyosis. Hum Reprod. 2016;31:734–49.
48. Shen M, Liu X, Zhang H, Guo SW. Transforming Growth Factor β1 Signaling Coincides with -Mediated Epithelial-Mesenchymal Transition and Fibroblast-to-Myofibroblast Transdifferentiation in Drive the Development of Adenomyosis in Mice. Hum Reprod 2016;In press.
49. Vigano P, Candiani M, Monno A, Giacomini E, Vercellini P, Somigliana E. Time to redefine endometriosis including its pro-fibrotic nature. Hum Reprod. 2018;33:347–52.
50. Chapron C, Tosti C, Marcellin L, Bourdon M, Lafay-Pillet MC, Millischer AE, et al. Relationship between the magnetic resonance imaging appearance of adenomyosis and endometriosis phenotypes. Hum Reprod. 2017;32:1393–401.
51. Marcellin L, Santulli P, Bortolato S, Morin C, Millischer AE, Borghese B, et al. Anterior focal Adenomyosis and bladder deep infiltrating endometriosis: is there a link? J Minim Invasive Gynecol. 2018;25:896–901.
52. Reid S, Lu C, Casikar I, Reid G, Abbott J, Cario G, et al. Prediction of pouch of Douglas obliteration in women with suspected endometriosis using a new real-time dynamic transvaginal ultrasound technique: the sliding sign. Ultrasound Obstet Gynecol. 2012;41:685–91.
53. Vercellini P, Buggio L, Borghi A, Monti E, Gattei U, Frattaruolo MP. Medical treatment in the management of deep endometriosis infiltrating the proximal rectum and sigmoid colon: a comprehensive literature review. Acta Obstet Gynecol Scand. 2018.

54. Szubert M, Zietara M, Suzin J. Conservative treatment of deep infiltrating endometriosis: review of existing options. Gynecol Endocrinol. 2018;34:10–4.
55. Yan D, Liu X, Guo S-W. Neuropeptides substance P and calcitonin gene related peptide accelerate the development and fibrogenesis of endometriosis. Sci Rep 2019;In press. .
56. Chiocchini ALC, Sportoletti C, Comai G, Brocchi S, Capelli I, Baraldi O, et al. Correlation between renal cortical stiffness and histological determinants by point shear-wave elastography in patients with kidney transplantation. Prog Transplant. 2017;27:346–53.